Correlation between mechanical properties and ionic conductivity of sodium superionic conductors: a relative density-dependent relationship

Eric Jianfeng Cheng[1]*, Tao Yang[1,2], Yuanzhuo Liu[1,2], Linjiang Chai[2], Regina Garcia-Mendez[3], Eric Kazyak[4], Zhenyu Fu[5], Guoqiang Luo[5], Fei Chen[5], Ryoji Inada[6], Vlad Badilita[7], Huanan Duan[8], Ziyun Wang[9], Jiaqian Qin[10], Hao Li[1], Shin-ichi Orimo[1,11], Hidemi Kato[11]

[1]Advanced Institute for Materials Research (WPI-AIMR), Tohoku University, Sendai 980-8577, Japan; [2]College of Materials Science and Engineering, Chongqing University of Technology, Chongqing 400054, China; [3]Department of Materials Science and Engineering, Johns Hopkins University, Baltimore, MD 21218 USA; [4]Department of Mechanical Engineering, University of Wisconsin-Madison, Madison, WI, 53706, USA; [5]State Key Laboratory of Advanced Technology for Materials Synthesis and Processing, Wuhan University of Technology, Wuhan 430070, China; [6]Department of Electrical and Electronic Information Engineering, Toyohashi University of Technology, Toyohashi, Aichi 441-8580, Japan; [7]Institute of Microstructure Technology, Karlsruhe Institute of Technology, Eggenstein-Leopoldshafen 76344, Germany; [8]State Key Laboratory of Metal Matrix Composites, School of Materials Science and Engineering, Shanghai Jiao Tong University, Shanghai 200240, China; [9]School of Chemical Sciences, University of Auckland, Auckland, New Zealand; [10]Metallurgy and Materials Science Research Institute, Chulalongkorn University, Bangkok, 10330, Thailand; [11]Institute for Materials Research, Tohoku University, Sendai, 980-8577, Japan

*Correspondence: ericonium@tohoku.ac.jp

Abstract

Sodium superionic conductors (NASICON) are pivotal for the functionality and safety of solid-state sodium batteries. Their mechanical properties and ionic conductivity are key performance metrics, yet their interrelation remains inadequately understood. Addressing this gap is vital for concurrent enhancements in both properties. This study summarizes recent literature on NASICON solid electrolytes $Na_{1+x}Zr_2Si_xP_{3-x}O_{12}$ (NZSP, $0 \leq x \leq 3$), highlighting the mechanical properties and ionic conductivity, and identifies a positive correlation between mechanical strength, in particular hardness, and ionic conductivity at ambient temperatures. Microstructural analysis reveals that a range of factors, including relative density, grain size, secondary phases, and crystallographic

structures, significantly influence material properties. Notably, an increase in relative density uniquely contributes to simultaneous enhancements in both ionic conductivity and mechanical strength. Consequently, future research should prioritize enhancing the relative density of NASICON solid electrolytes, possibly employing advanced techniques, including sol-gel process, spark plasma sintering (SPS), and microwave-assisted sintering. The correlation between mechanical properties and ionic conductivity observed in NASICON solid electrolytes extends to other high-temperature sintered oxide electrolytes like $Li_7La_3Zr_2O_{12}$ (LLZO). This investigation not only suggests a potential linkage between these crucial properties but also guides subsequent strategies for refining solid electrolytes for advanced battery technologies.

1. Introduction

In the early 21st century, environmental considerations have become increasingly critical, profoundly influencing economic progression and human sustainability. The advent of international agreements such as the Kyoto Protocol and the Paris Agreement mark a global commitment to diminishing carbon emissions, catalyzing a shift from traditional fossil fuels to renewable energy sources. This transformation is imperative in addressing climate change and promoting sustainable development.

The intermittent nature of renewable energy sources, such as solar and wind, necessitates the integration of reliable electrochemical energy storage systems within future electrical grids. These systems are pivotal in managing intermittency and ensuring a stable energy supply. The primary energy storage technologies include lead-acid, nickel-cadmium, nickel-metal hydride, lithium-ion, and sodium-sulfur batteries [1]. Among these, sodium-ion batteries stand out due to their cost-effectiveness and reliable performance, garnering significant attention in academia and industry [2-3].

A critical aspect of these batteries is safety, an area where solid-state electrolytes (SSEs) demonstrate considerable promise. Traditional organic liquid electrolytes are susceptible to leakage, electrode corrosion, and risks of combustion and explosion under high temperatures. In contrast, inorganic SSEs can fundamentally mitigate these safety issues, elevating the overall safety profile of batteries due to their non-volatility, mechanical and thermal stability, and low flammability [2-6]. Additionally, SSEs serve dual functions as both electrolytes and separators, which could simplify battery architecture and reduce packaging costs [7]. Consequently, the research on SSEs has emerged

as a focal point in the advancement of secondary battery technologies.

The historical development of SSEs can be traced back to the early 19th century. Michael Faraday's seminal discovery of Ag_2S and PbF_2 in 1830, which demonstrated metal-like ionic conductivity at elevated temperatures (177-500 °C), laid the foundational groundwork for the field of solid-state ionics (SSI). This pioneering work was further advanced in 1923 with the discovery of monoclinic, halogen-containing SSEs, exemplified by $LiAlCl_4$, marking a notable progression in SSI. The subsequent period, notably in 1930, saw focused research on substituting halogen elements in the composition of SSEs (LiX, where X= F, Cl, Br, I) to enhance their ionic conductivity at room temperature (RT) [8].

The trajectory of SSE development took a significant turn in 1960 with the introduction of the Ag_3SI electrolyte, which exhibited considerable RT ionic conductivity of 1×10^{-2} S/cm. This development was crucial as it led to the assembly of solid-state batteries ($Ag/Ag_3SI/I_2$), effectively addressing the flammability issues associated with organic liquid electrolytes [9-11]. Further advancements were made in 1967 with the $Na_2O\cdot11Al_2O_3$ electrolyte (beta-alumina), recognized for its high Na^+ ionic conductivity (10^3 S cm^{-1} at 300 ºC) and its application in Na-S batteries [12-13]. A pivotal breakthrough occurred in 1976 when Hong and Goodenough synthesized a promising sodium-ion inorganic SSE, $Na_{1+x}Zr_2Si_xP_{3-x}O_{12}$ (NZSP, $0\leq x\leq3$) [14]. NZSP, a solid solution derived from $NaZr_2P_3O_{12}$ (NZP) and $Na_4Zr_2Si_3O_{12}$ (NZS), with Si partially substituting for P to maintain charge balance, has garnered considerable attention due to its high RT ionic conductivity (up to 6.7×10^{-4} S/cm), stable three-dimensional structure, wide electrochemical window (> 5V *vs.* Na/Na^+), high thermal stability, non-reactivity with Na, high decomposition pressure, and moisture insensitivity [2, 15-16]. However, its RT ionic conductivity still falls short of practical application requirements, primarily due to the standard set for NASICON SSEs, which often need to exceed 10^{-1} mS/cm [2]. Consequently, enhancing the RT ionic conductivity of SSEs has become a central focus of contemporary research. Since 2010, various studies have reported significant progress in this area through the optimization of composition (adjusting the *x* value and ionic doping) and processing conditions (modifying sintering parameters, employing novel techniques, and adding sintering aids). These advancements have enabled the RT ionic conductivity of these electrolytes to meet or even surpass the required standards for practical applications [7, 17-21]. Figure 1 captures the developmental

history of NASICON SSEs, illustrating the chronological advancements in this evolving field.

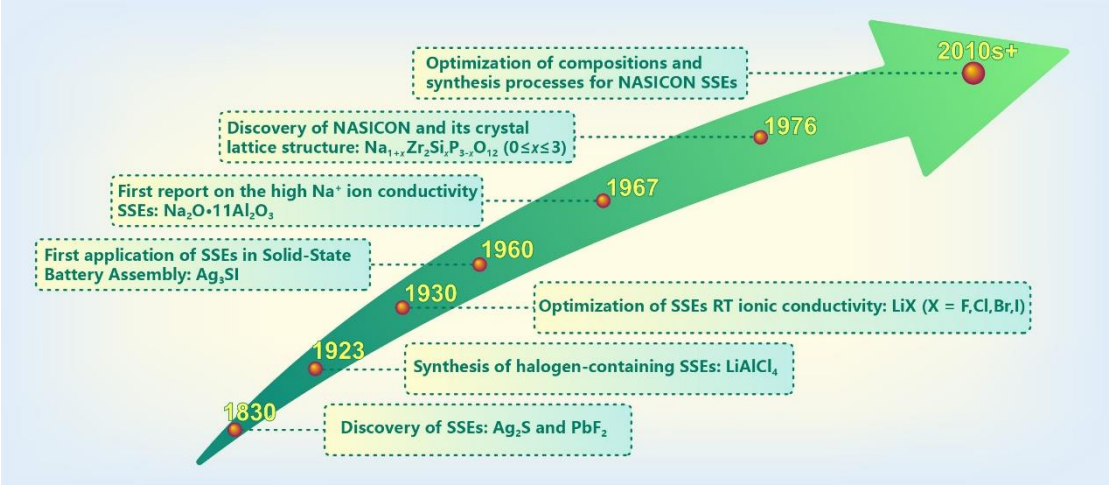

Fig. 1. A succinct history of NASICON solid electrolytes

Recent studies have underscored the limitations of focusing exclusively on high ionic conductivity to ensure long-term stability and safety of sodium batteries using NASICON electrolytes. In practical applications, these electrolytes will inevitably encounter challenges such as metal dendrite growth and crack formation and propagation, leading to electrolyte failure [20, 22]. Addressing these challenges necessitates that SSEs not only conduct ions but also possess robust mechanical properties, wide electrochemical windows and chemical stability against electrodes. Specifically, mechanical properties are vital to ensure structural integrity upon cycling, potentially preventing uncontrolled penetration of metal dendrites, thus maintaining battery safety and performance [2, 23-26].

The formation of metal dendrites within SSEs is a complex phenomenon that transcends the bounds of classical mechanics. Monroe et al. proposed that the growth of metal dendrites could be effectively mitigated by ensuring that the shear modulus of the SSEs is at least twice as high as that of the metallic anode [27]. However, experimental studies have extensively demonstrated metal dendrite formation in ceramic SSEs, even where the shear modulus markedly surpasses that of the metallic anode [28-30]. Moreover, the role of electronic conductivity within SSEs has been identified as a critical factor influencing metal dendrite growth [31]. Despite these complexities, enhancing the mechanical properties of SSEs remains a viable strategy for the physical suppression of metal dendrite proliferation in solid electrolytes.

The mechanical properties of NASICON electrolytes also hold significant importance for the

manufacturing and functionality of solid-state batteries (SSBs). Specifically, the operation of SSBs benefits from a higher fracture toughness in electrolytes, as it permits the use of thinner layers, thereby reducing resistance and enhancing energy density. Furthermore, empirical evidence indicates a positive correlation between fracture toughness and critical current density, with the critical current density increasing alongside the fracture toughness [32-33]. Additionally, addressing the occurrence of micro-cracking in SSEs has been found to link to the improvement in ductility [34]. As a result, the examination of NASICON electrolytes' mechanical properties has emerged as a critical area of research [7, 17-21, 35-37].

Wolfenstine et al. [38] provided a comprehensive summary of the primary mechanical properties of NASICON electrolytes, which include hardness (4.4-4.9 GPa), elastic modulus (56-97 GPa), fracture toughness (1-1.5 $MPa \cdot m^{0.5}$), and fracture strength (50-110 MPa). Recent investigations have broadened our understanding of these properties, significantly enriching the data pool necessary for establishing a correlation between mechanical properties and ionic conductivity.

In the quest for high-performance solid-state batteries, the manufacturing of SSEs that exhibit superior ionic conductivity and mechanical properties is paramount. Despite advancements in developing NASICON electrolytes with enhanced mechanical or electrical characteristics through various methodologies, a holistic examination of strategies to concurrently improve both attributes remains a crucial need. This study addresses two fundamental inquiries: the existence of a direct correlation between the mechanical properties and ionic conductivity of NASICON SSEs, and the strategies for concurrent improvement of these characteristics in future research. Through an extensive analysis of existing experimental data, this work elucidates key parameters indicative of these properties, explores their interrelationship, and compiles principal factors influencing them. The findings offer insightful direction for the future development or selection of SSEs with optimized integrated performance.

2. Current research status on the mechanical properties of NASICON

The mechanical properties of NASICON electrolytes, including hardness, elastic modulus, fracture strength, and fracture toughness, are crucial in preventing crack propagation, suppressing dendrite growth, and maintaining a stable interface with a Na metal electrode [38]. Consequently, SSEs must not only possess high ionic conductivity but also adequate mechanical properties to guarantee

operational durability and stability. Recently, an increasing number of scholars have started to investigate both the mechanical properties and ionic conductivity of NASICON concurrently. This integrative approach is significant, as it offers a more holistic understanding of electrolyte performance. Despite this growing interest, there is still a notable scarcity of research directly exploring the interplay between these two critical properties. Table 1 provides a comprehensive overview of the existing research data, effectively contrasting the mechanical properties with the ionic conductivity of NASICON electrolytes.

In examining the evolution of research on NASICON electrolytes, it is noteworthy that Nonemacher et al. initially characterized their mechanical properties in 2019 [14]. This seminal work has catalyzed a growing interest in the field, evidenced by a consistent annual increase in related research. The predominant strategies to enhance the mechanical properties of NASICON electrolytes encompass a variety of approaches: doping [17-19], compositional modification [7], incorporation of sintering aids [20], and use of more-recently broadly adopted fabrication techniques such as microwave-assisted sintering [39] and a hybrid fabrication method that combines tape-casting and hot-pressing [35]. These methodologies have been instrumental in significantly improving the mechanical robustness of NASICON electrolytes. Additionally, the RT total ionic conductivities documented in various studies exhibit a notable range, spanning from 0.1 to 5 mS/cm, which underscores the generally high ionic conductivity of NASICON electrolytes [2].

Recent studies on NASICON electrolytes have predominantly concentrated on their mechanical properties, with specific attention to hardness [7, 17-21, 35], elastic modulus (Young's modulus) [17-18, 20-21], bending strength, and fracture toughness [17, 21]. Notably, the latest measurements for hardness and elastic modulus have exceeded the ranges previously summarized by Wolfenstine et al. [38] in 2022, which were 4.4-4.9 GPa for hardness and 56-88 GPa for elastic modulus. Furthermore, the literature reveals significant variations in the reported ionic conductivity and mechanical properties of NASICON electrolytes, yet a definitive correlation between these parameters remains elusive. Given that hardness is a fundamental mechanical characteristic of NASICON electrolytes, which shows a positive correlation with the elastic modulus [38] and is comparatively simpler to measure than other mechanical properties, it has become a primary focus of research. Furthermore, the hardness of a NASICON solid electrolyte serves as an indicator of its

relative density, which in turn is fundamentally associated with its ionic conductivity. Consequently, this study aims to elucidate the relationship between room temperature hardness and total ionic conductivity in NASICON electrolytes, thereby shedding light on the interplay between ionic conductivity and mechanical properties.

Table 1 Mechanical properties and RT total ionic conductivity of NASICON solid electrolytes

Compound	Sintering condition	Secondary phase/impurity	Grain size (μm)	Relative density (%)	Mechanical properties						RT Total Ion Conductivity (mS/cm)	Ref.
$Na_3Zr_2Si_2PO_{12}$	1200 °C-0.5 h +1150 °C-5 h	ZrO_2	/	85~93	Vickers Hardness (HV)	734.7	Elastic Modules (GPa)	88	Fracture Toughness ($MPa·m^{1/2}$)	1.5	1.7	Nonemacher et al. 2019 [17]
$Na_{3.1}Al_{0.05}Y_{0.05}Zr_{1.9}Si_2PO_{12}$						693.9		83		1.55	1.6	
$Na_{3.2}Al_{0.1}Y_{0.1}Zr_{1.8}Si_2PO_{12}$						561.2		73		1.59	1.3	
$Na_{3.4}Al_{0.2}Y_{0.2}Zr_{1.6}Si_2PO_{12}$						673.5		75		1.58	1.4	
$Na_{3.6}Al_{0.3}Y_{0.3}Zr_{1.4}Si_2PO_{12}$						602.0		79		1.35	0.46	
$Na_3Zr_2Si_2PO_{12}$	1050 °C-12 h	$Na_2ZrSi_2O_7$, ZrO_2, SiO_2	/	92.4	Vickers Hardness (HV)	232.7	Young's modulus (GPa)	54.4	/		0.285	Luo et al. 2022 [18]
$Na_{3+x}Zr_{1.9}Co_{0.1}Si_2PO_{12}$		$Na_2ZrSi_2O_7$, ZrO_2		90.9		117.3		48			0.333	
$Na_{3+x}Zr_{1.8}Co_{0.2}Si_2PO_{12}$		$Na_2ZrSi_2O_7$, ZrO_2		86.6		138.8		37			0.389	
$Na_{3+x}Zr_{1.7}Co_{0.3}Si_2PO_{12}$		$Na_2ZrSi_2O_7$, ZrO_2, SiO_2, $Na_6Si_2O_7$		85.6		123.5		36			0.457	
$Na_{3+x}Zr_{1.9}Fe_{0.1}Si_2PO_{12}$		$Na_2ZrSi_2O_7$, ZrO_2		92.8		243.9		60			0.372	
$Na_{3+x}Zr_{1.8}Fe_{0.2}Si_2PO_{12}$		$Na_2ZrSi_2O_7$, ZrO_2		92.8		439.8		79			0.390	
$Na_{3+x}Zr_{1.7}Fe_{0.3}Si_2PO_{12}$		$Na_2ZrSi_2O_7$, ZrO_2		93.1		495.1		80.3			0.513	
$Na_{3+x}Zr_{1.9}Ni_{0.1}Si_2PO_{12}$		$Na_2ZrSi_2O_7$		89.3		103.1		38			0.558	
$Na_{3+x}Zr_{1.8}Ni_{0.2}Si_2PO_{12}$		$Na_2ZrSi_2O_7$, ZrO_2		85.2		106.1		37.5			0.443	
$Na_{3+x}Zr_{1.7}Ni_{0.3}Si_2PO_{12}$		$Na_2ZrSi_2O_7$, ZrO_2, SiO_2, $Na_6Si_2O_7$, $Ni_3(PO_4)_2$		85.4		110.2		38			0.113	
$Na_3Zr_2Si_2PO_{12}$	1250 °C-1 h	Amorphous phase, ZrO_2	0.5−3	92.1	Bend strength (MPa)	73	/				0.51	Go et al. 2021 [7]
$Na_{3.1}Zr_{1.55}Si_{2.3}P_{0.7}O_{11}$		Amorphous phase, ZrO_2	2−6	91.7		95					1.4	
$Na_3Zr_2Si_2PO_{12}$	1100 °C-12 h	ZrO_2	>1	88.4	Vickers Hardness (HV)	291	/				0.39	Ran et al. 2021 [19]
$Na_{3.1}Zr_{1.8}Sc_{0.1}Ge_{0.1}Si_2PO_{12}$			<1	91.1		/					1.61	
$Na_{3.125}Zr_{1.75}Sc_{0.125}Ge_{0.125}Si_2PO_{12}$				99.7		505					4.64	
$Na_{3.15}Zr_{1.7}Sc_{0.15}Ge_{0.15}Si_2PO_{12}$				95.7		/					1.89	
$Na_3Zr_2Si_2PO_{12}$	1180 °C-12 h	/	1.4	86.7	Vickers Hardness (HV)	346.9	Young's modulus (GPa)	55.5	/		0.61	Gao et. al. 2022 [20]
$Na_3Zr_2Si_2PO_{12}$+2 wt% TiO_2		TiO_2	1.9	95.9		949.0		92.2			0.66	
$Na_3Zr_2Si_2PO_{12}$	1050 °C-5 min (SPS)	$Na_2ZrSi_4O_{11}$, $ZrSiO_4$, SiO_2	/	90	Vickers Hardness (HV)	673.5	Elastic Modules (GPa)	82	Fracture Toughness ($MPa·m^{1/2}$)	2.1	0.34	Hitesh et al. 2023 [21]
	1050 °C-10 min (SPS)		/	94		357.1		77		2.8	0.35	
	1050 °C-20 min (SPS)		17	97.4		540.8		81		2.3	0.45	
	1050 °C-20 min (SPS)+1100 °C-5 h (annealing)	$Na_2ZrSi_4O_{11}$	46	97.9		469.4		81.5		1.9	/	
	1050 °C-20 min (SPS)+1100 °C-10 h (annealing)	$Na_2ZrSi_4O_{11}$	42	98		510.2		79.9		1.8	highest in annealed samples	
	1050 °C-20 min (SPS)+1100 °C-20 h (annealing)	$Na_2ZrSi_4O_{11}$	52	96.1		693.9		86.7		2.6	/	
	1050 °C-20 min (SPS)+1100 °C-40 h (annealing)	$Na_2ZrSi_4O_{11}$	71	96.5		581.6		84.8		2.2	/	
$Na_{3.16}Zr_{1.84}Y_{0.16}Si_2PO_{12}$	1200 °C-10 h (hot-pressing)	Na_3PO_4、ZrO_2	<1	90	Vickers Hardness (HV)	325	/		/		0.1	Naranjo-Balseca et al. 2023 [35]

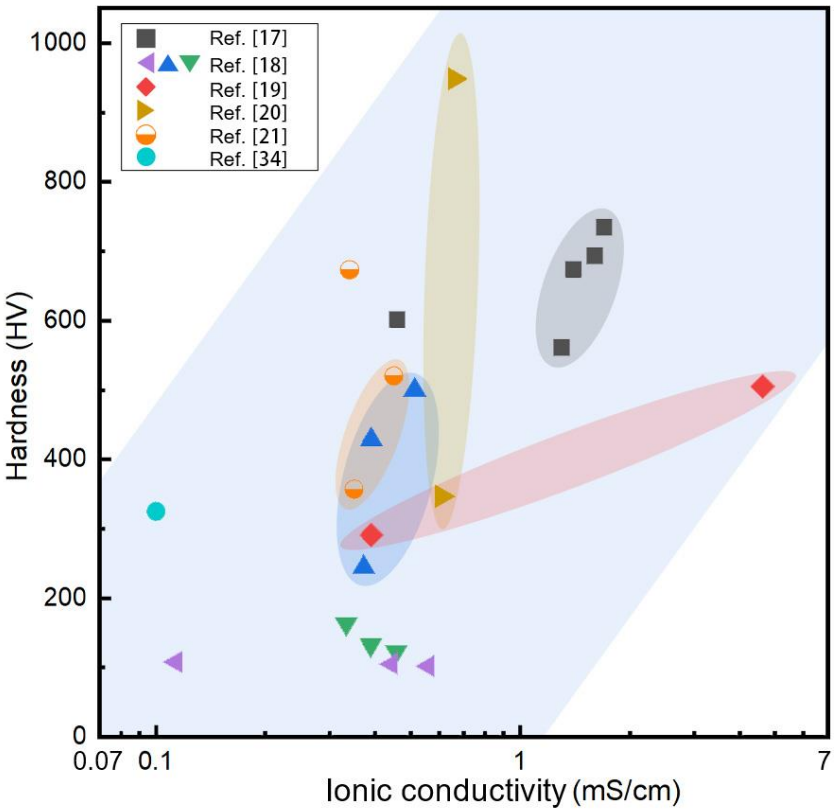

Fig. 2 Correlation between total ionic conductivity and hardness at RT. The data are sourced from references [17-21, 35]. Identical symbols indicate samples obtained by varying a specific condition to achieve different ionic conductivities and hardnesses. The gray squares represent doping with different contents of Al and Y [17]; purple, blue, and green triangles represent doping with varying amounts of Ni, Fe, and Co, respectively [18]; red diamonds represent doping with Sc and Ge [19]; brownish-yellow triangles represent the addition of TiO_2 [20]; and orange semicircles represent different SPS sintering durations [21]. Samples denoted by ellipses of the same color indicate a positive correlation between their hardness and ionic conductivity.

In Figure 2, a comparative analysis of the interrelationship between the total ionic conductivity and hardness of NASICON electrolytes is presented. This plot illustrates a predominant trend where an enhancement in ionic conductivity corresponds to an increase in material hardness. This is particularly evident in studies where a single parameter is varied (denoted by consistent color and

symbol representation), with most materials (highlighted within ellipses) demonstrating this trend. Conversely, a minority of specimens display a marginal reduction in hardness concurrent with increased ionic conductivity. The comprehensive analysis of the collected data indicates that most specimens exhibiting increased ionic conductivity consistently demonstrate enhanced hardness values. This pattern indicates a tentative positive correlation between the ionic conductivity and the hardness of these electrolytes. The subsequent section will delve into a detailed exploration of the underlying mechanisms potentially driving this positive correlation.

3. Correlation between mechanical properties and ionic conductivity

The intrinsic connection between the mechanical properties and ionic conductivity of NASICON electrolytes, as briefly discussed earlier, stems from their microstructural characteristics. The mechanical properties of NASICON electrolytes are predominantly determined by factors including relative density, crystal structure, the presence of secondary phases, the content of solute elements, bond strength, and grain size. In parallel, ionic conductivity is similarly influenced by variables such as relative density, crystal structure, sodium ion concentration, secondary phases, carrier mobility, and grain size. This shared dependence on microstructural elements underscores the fundamental correlation between the mechanical and ionic properties of NASICON electrolytes. The subsequent sections are dedicated to an in-depth analysis of trends in both mechanical properties and ionic conductivity, with a particular focus on their microstructural underpinnings. Moreover, the study highlights various measures, such as processing techniques, doping methods, and sintering aids, that impact these properties. The aim is to provide a comprehensive guide for future research endeavors seeking to synergistically enhance both the mechanical properties and ionic conductivity of NASICON electrolytes.

3.1 Relative Density

Relative density significantly influences the mechanical properties of NASICON electrolytes.

A higher relative density corresponds to reduced pore defects and more compact grain contact, thereby diminishing the likelihood of material plastic deformation or fracture due to stress concentration under loading conditions. This enhancement in relative density also promotes a more efficient flow of Na ions, leading to increased ionic conductivity. SEM microstructures depicted in Fig. 3 demonstrate that with an increase in density, there is a concurrent rise in both hardness and ionic conductivity of the NZSP solid electrolyte. Therefore, it is imperative for future research to focus on improving material density, as this could synergistically improve both aforementioned properties.

The conventional preparation method, i.e., high-temperature and pressure-less sintering, is straightforward and scalable. However, they often result in NASICON electrolytes characterized by a high concentration of defects, such as pores , yielding lower relative densities of slightly higher than 90% [21]. Employing a mechanochemically assisted solid-state method enhances the densification of pellets during sintering, but this approach concurrently introduces disordering and partial amorphization to the particle surface [40]. In response to this challenge, research has shifted towards exploring alternative fabrication processes for NASICON electrolytes. Techniques such as sol-gel, which facilitates uniform precursor mixing at the molecular level, and spark plasma sintering (SPS), known for its rapid densification capabilities through microdischarges between particles, have successfully produced NASICON solid-state electrolytes (SSEs) with notably higher relative densities of approximately 98% or even higher [21, 41-44]. Moreover, employing a polydisperse particle size distribution in the sintering process can improve the compactness of NASICON solid electrolytes [40].

Furthermore, the inclusion of low-melting-point sintering aids in the precursor mixture has become a common practice for relative density optimization. This strategy leverages the liquid phase formed from the sintering aids to fill gaps among precursor particles. As the concentration of

sintering aids increases, densification improves initially; beyond a certain threshold, it decreases due to the emergency of voids within the material. Thus, an optimal amount of sintering additives is crucial for promoting material densification and facilitating substance transport. Sintering additives, such as NaF [45], NaBr [46], Na_3BO_3 [47], $NaPO_3$ [48], Na_2SiO_4 [49], Na_2O-Nb_2O_5-P_2O_5 [43], B_2O_3 [50], and La_2O_3 [51], have demonstrated considerable effectiveness in enhancing the relative density of NASICON solid electrolytes.

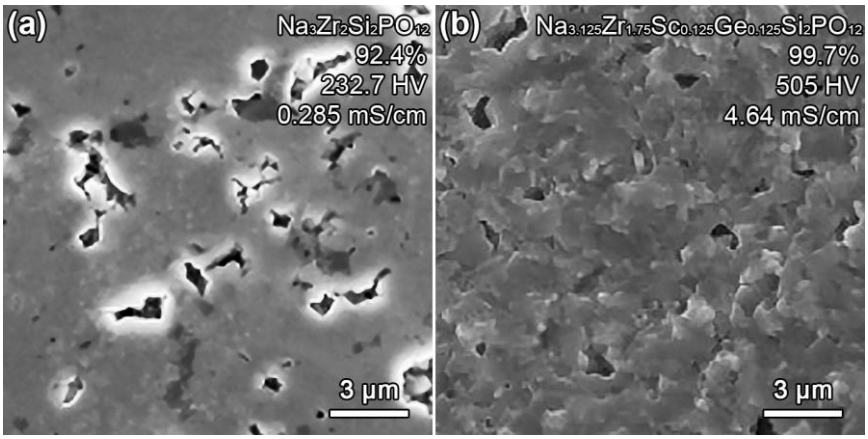

Fig. 3 SEM microstructures of typical NASICON electrolytes with different relative densities reported in the literature, along with corresponding ionic conductivity and hardness data: (a) $Na_3Zr_2Si_2PO_{12}$ [18]; (b) $Na_{3.125}Zr_{1.75}Sc_{0.125}Ge_{0.125}Si_2PO_{12}$ [19].

3.2 Grain sizes

The interplay between grain size and its dual impact on ionic conductivity and mechanical properties in polycrystalline solid electrolytes presents a complex, "double-edged sword" phenomenon. On the one hand, refining grain size contributes to enhanced mechanical properties through grain refinement strengthening. It is also important to recognize that excessive grain growth is detrimental to the enhancement of electrolyte densification. Conversely, refinement of grains results in a higher volume fraction of grain boundaries. Refined grains are typically characterized by an increased concentration of defects along these grain boundaries. The increase of grain boundaries and associated defects tends to increase grain boundary resistance and decrease ionic

conductivity, as discussed in the literature [7].

Given this intricate relationship, achieving precise control over grain size is crucial in the design and optimization of crystalline solid electrolytes. Such control is especially vital for maintaining a balance between ionic conductivity and mechanical integrity. This balance is evident in the sintering process, where grain size is a direct function of the sintering duration. Extended holding times during sintering are known to produce larger grains [21]. Consequently, tailoring the holding times across various sintering techniques, such as solid-phase sintering, hot-pressing, and SPS, becomes a critical strategy. This approach effectively aligns the preservation of sufficient ionic conductivity with the enhancement of mechanical properties [21, 41].

3.3 Secondary phases

The secondary phases in NASICON electrolytes play a dual role, similar to grain size in influencing mechanical properties and ionic conductivity. The formation of hard, fine secondary phases like ZrO_2 enhances mechanical strength through secondary phase strengthening. However, the formation of secondary phases often results in a notable reduction in ionic conductivity due to the negligible transport of sodium ions through these phases. This decrease is attributed to the generally low ionic conductivity of the secondary phase and the introduction of new grain boundary resistance [7]. Typical secondary phases in NASICON include ZrO_2, SiO_2, $Na_2ZrSi_4O_{11}$, $ZrSiO_4$, $Na_6Si_2O_7$, and amorphous phases [18, 21, 41]. These phases predominantly arise from incomplete crystallization during NASICON sintering. This incomplete process, often due to Na and P element volatilization at high temperatures, results in a deviation from the stoichiometric $Na_3Zr_2Si_2P_3O_{12}$, leading to new phase formation. While these impure phases can enhance mechanical properties, they also potentially cause microcracking in NASICON electrolytes, particularly due to stress concentration during the post-sintering cooling process, thereby impairing mechanical strength [7].

To mitigate the formation of these secondary phases, two primary strategies are currently

employed. The first involves adding excessive Na and P elements, such as Na_2CO_3 [20], $(NH_4)_2HPO_4$ [18], or Na_3PO_4 [21], and covering the pellets with NASICON powder during conventional sintering [35]. The second strategy includes adopting novel processes that lower sintering temperatures, thus reducing Na and P volatilization. These include the sol-gel preparation of liquid-phase precursors prior to sintering [32, 40] and sintering powder precursors using SPS [42-43]. Both approaches have successfully lowered the processing temperature by approximately 200 °C, significantly minimizing the likelihood of secondary-phase formation [41-43, 52]. Meanwhile, the composition of the secondary phases can be precisely regulated through the incorporation of targeted sintering additives or elemental dopants. For example, La_2O_3 was used as a sintering aid to modulate the chemical composition at the grain boundaries and induce the formation of the second phase $Na_3La(PO_4)_2$, which not only increased the ionic conductivity of NZSP and but also enhanced the relative density [51]. Similarly, the introduction of Al into the Si/P sites led to an increased formation of the secondary phase Na_3PO_4 at the grain boundary. This resulted in noticeable decrease of the grain boundary resistance [53].

3.4 Crystal structure

NASICON, characterized by a unique three-dimensional phosphate structure, facilitates Na^+ migration. Its formula, $Na_{1+x}Zr_2Si_xP_{3-x}O_{12}$ (where $0 \leq x \leq 3$), varies based on the degree of Si substitution for P. The crystal structure of NASICON shifts with different doping levels of x. Specifically, a rhombohedral structure is observed for $0 \leq x < 1.8$ and $2.2 < x \leq 3$, while a monoclinic phase occurs at $1.8 \leq x \leq 2.2$, as depicted in Fig. 4 [14, 54]. The rhombohedral phase, being more symmetric and less distorted than the monoclinic phase, demonstrates a lower activation energy for Na^+ diffusion, resulting in enhanced RT ionic conductivity (approximately 0.1-1 mS/cm) [7, 19, 44] Conversely, the highest ionic conductivity in monoclinic NASICON electrolytes (about 0.67 mS/cm) is noted at $x = 2$ [55].

The transition between these crystal structures not only affects ionic conductivity but also mechanical properties. The monoclinic phase, due to its lower symmetry and greater lattice distortion, exhibits slightly increased hardness. Nonemacher et al. observed a gradual hardness reduction in NZSP transitioning from the monoclinic to the rhombohedral phase [17]. This suggests a trade-off between mechanical properties and ionic conductivity in NASICON. However, this trade-off may not necessitate compromising the ionic conductivity of the rhombohedral phase for enhanced mechanical properties, as it already exhibits high hardness (5-7 GPa) and elastic modulus (75-85 GPa) [17].

Enhancement of the rhombohedral phase has been achieved through various methods. These include lowering the phase transition temperatures from monoclinic to rhombohedral through Ge doping [56], increasing the stability of the rhombohedral phases via Sc doping [17], and altering the value of x (e.g., x=2.3) to increase the content of the rhombohedral phase [7]. In addition, doping NASICON electrolytes with various elements can alter the ratio between monoclinic and rhombohedral structures, simultaneously causing changes to the volume of crystal cells. These changes significantly influence the electrolytes' mechanical properties and conductivity. For example, introducing bivalent elements like Zn^{2+} and Mg^{2+} [57] or tetravalent elements such as Hf^{4+} [51], increases the rhombohedral phase proportion and enlarges the bottleneck size in Na^{+} migration pathways, facilitating higher Na^{+} mobility. However, when substitutive ions (such as Nd^{3+} and Co^{2+}) have radii substantially larger or smaller than Zr^{4+} (0.72 Å) [58], their integration into crystal lattice becomes problematic, hindering potential conductivity enhancement [45].

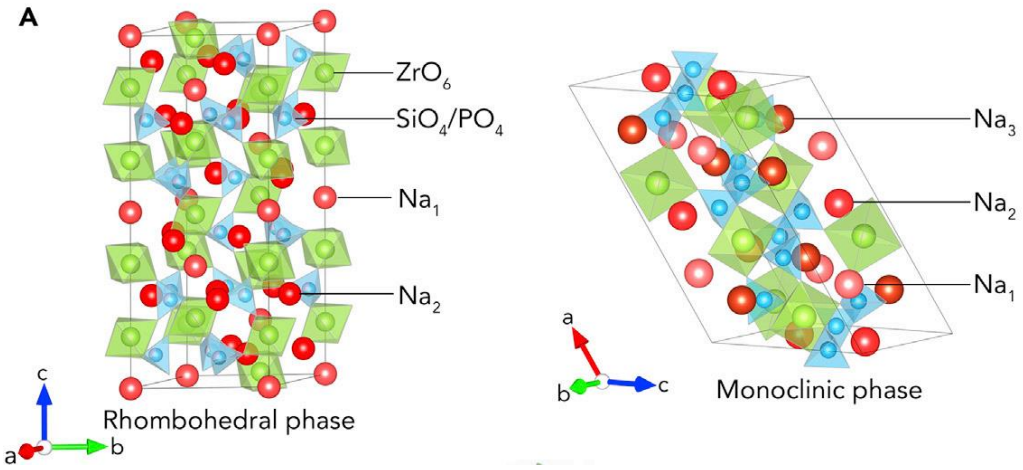

Fig. 4. Two typical NASICON crystal structures [59]

Figure 5 presents an analysis of four key factors influencing the properties of NASICON electrolytes. This analysis reveals a trade-off relationship between ionic conductivity and mechanical properties for all factors except relative density. The study suggests that enhancing the relative density of NZSP electrolytes is crucial for simultaneously improving both their mechanical properties and ionic conductivity, assuming that coarsening is prevented during processing. This hypothesis is further supported by the data in Figure 6, which demonstrates a positive correlation between density, hardness, and ionic conductivity in NASICON electrolytes, as evidenced in literature. Notably, higher densities are consistently linked with increased hardness and ionic conductivity, validating our initial hypothesis. While increasing density synergistically enhances both properties, the other three factors predominantly contribute to a trade-off between them. Consequently, future research on NASICON electrolytes' sintering preparation should prioritize augmenting relative density. Subsequent efforts should focus on achieving an optimal balance between ionic conductivity and mechanical properties through additional processing techniques. However, it should be noted that the significant hardness of NASICON electrolytes adversely affects the maintenance of effective interfacial contact with electrode materials, particularly cathode materials. Conversely, softer Na-ion conductive solid electrolytes, such as the complex hydride $Na_2B_{10}H_{10}$-$Na_2B_{12}H_{12}$, offer advantages in addressing the issue of interfacial contact [60-61].

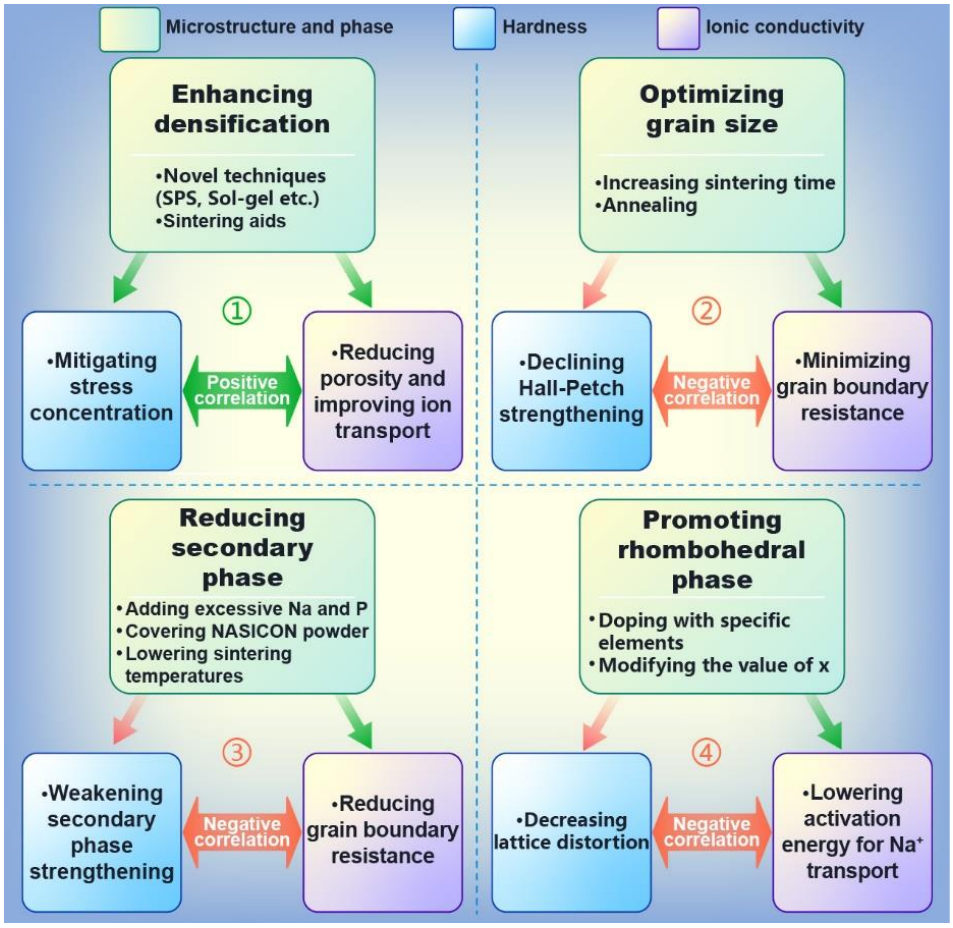

Fig. 5 Summary of key factors influencing both hardness and ionic conductivity in NASICON solid electrolytes.

Furthermore, the correlation between mechanical properties and ionic conductivity observed in sodium superionic conductors is applicable to other high-temperature sintered hard ceramic electrolytes, such as lithium superionic conductors—$Li_7La_3Zr_2O_{12}$ (LLZO) and $Li_{1.3}Al_{0.3}Ti_{1.7}(PO_4)_3$ (LATP) [62-63]. Specifically, LLZO demonstrates that an increase in hardness correlates with enhanced ionic conductivity. For instance, the ionic conductivity of LLZO at room temperature (RT) improves from 0.0094 to 0.34 mS/cm, and its Vickers hardness escalates from 4.7 to 9.1 GPa as the relative density rises from 85% to 98% [63].

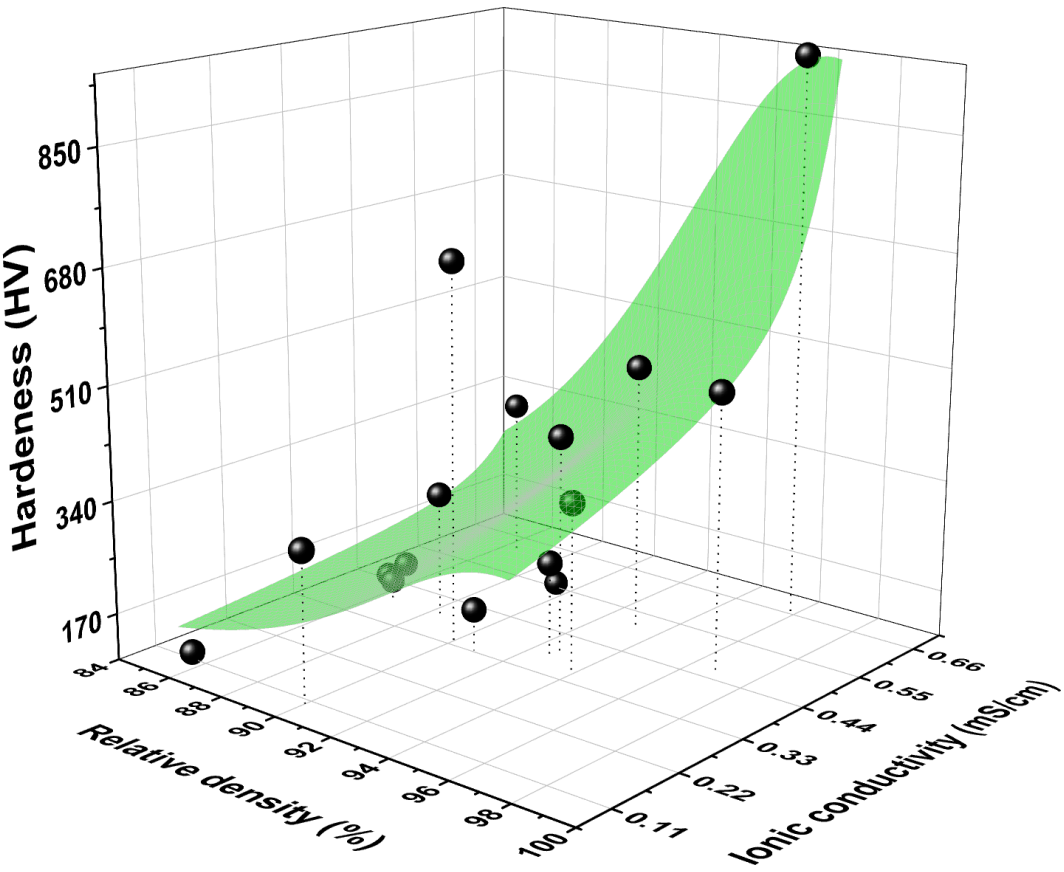

Fig. 6. Correlation of relative densities with room-temperature ionic conductivity, and hardness (Data adapted from Ref. [59])

4. Conclusion and future perspective

This study delves into the mechanical properties and ionic conductivity of NASICON solid electrolytes, two of their fundamental characteristics. An extensive review and analysis of the current literature reveals a generally positive correlation between these two properties, particularly emphasizing the link between hardness (a major mechanical property) and ionic conductivity. The correlation primarily stems from several factors, including relative density, grain size, secondary phases, and crystal structure. Among these, relative density emerges as the most decisive in determining the relationship between ionic conductivity and hardness. The other factors demonstrate a trade-off effect. Consequently, the advancement of NASICON electrolytes should

prioritize enhancing the relative density, leveraging techniques like sol-gel, SPS, and the incorporation of sintering aids. Achieving a high relative density allows for subsequent refinements (e.g., increasing grain size through annealing), aiming to optimize the balance between the ionic conductivity and mechanical properties for future development of solid electrolytes. The observed correlation between mechanical properties and ionic conductivity in sodium superionic conductors is also applicable to high-temperature sintered lithium superionic conductors. The mechanical properties of SEs are crucial for the optimal performance of solid-state batteries. These properties significantly influence interfacial compatibility, the formation and evolution of micro-cracks and voids, and the growth and propagation of metal dendrites, alongside the well-recognized importance of ionic conductivity.

We will further explore the correlation between mechanical properties and conductivity through various characterization and computational methods to provide more conclusive correlated results in the future. For example, temperature-dependent sodium (Na) NMR spectroscopy has been employed to examine the locational movement of Na^+ ions, providing insights into the ions' average hopping rate and the activation energy barriers [64]. Despite its potential, NMR spectroscopy has been relatively underexploited in obtaining information related to the mechanical strength of NASICON materials. However, given NMR's capability to offer insights across multiple length scales down to atomic level, it is hypothesized that NMR spectroscopy could yield valuable constitutive material information that may be directly utilized to ascertain mechanical properties or serve as input for various computational models to predict these properties.

Acknowledgements

This research was financially supported by Core Research Cluster for Materials Science (CRC-MS) of Tohoku University, Ensemble Grants for Early Career Researchers 2023 of Tohoku University,

GIMRT program of the Institute for Materials research of Tohoku University (Proposal Number: 202308-CRKKE-0221), AIMR Fusion Research program 2023 of the Advanced Institute for Materials Research of Tohoku University, and TEPCO Memorial Foundation.

References

1. Guin, M.; Tietz, F., Survey of the transport properties of sodium superionic conductor materials for use in sodium batteries. *J. Power Sources* **2015,** *273*, 1056-1064.

2. Li, Y.; Li, M.; Sun, Z.; Ni, Q.; Jin, H.; Zhao, Y., Recent advance on NASICON electrolyte in solid-state sodium metal batteries. *Energy Storage Mater.* **2023,** *56*, 582-599.

3. Hueso, K. B.; Palomares, V.; Armand, M.; Rojo, T., Challenges and perspectives on high and intermediate-temperature sodium batteries. *Nano Res.* **2017,** *10* (12), 4082-4114.

4. Cheng, E. J.; Kushida, Y.; Abe, T.; Kanamura, K., Degradation Mechanism of All-Solid-State Li-Metal Batteries Studied by Electrochemical Impedance Spectroscopy. *ACS Appl. Mater. Interfaces* **2022,** *14* (36), 40881-40889.

5. Shoji, M.; Cheng, E. J.; Kimura, T.; Kanamura, K., Recent progress for all solid state battery using sulfide and oxide solid electrolytes. *J. Phys. D: Appl. Phys.* **2019,** *52* (10), 103001.

6. Cheng, E. J.; Oyama, R.; Abe, T.; Kanamura, K., High-voltage all-solid-state lithium metal batteries prepared by aerosol deposition. *J. Eur. Ceram. Soc.* **2023,** *43* (5), 2033-2038.

7. Go, W.; Kim, J.; Pyo, J.; Wolfenstine, J. B.; Kim, Y., Investigation on the Structure and Properties of $Na_{3.1}Zr_{1.55}Si_{2.3}P_{0.7}O_{11}$ as a Solid Electrolyte and Its Application in a Seawater Battery. *ACS Appl. Mater. Interfaces* **2021**, 52727-52735.

8. He, B.; Zhang, F.; Xin, Y.; Xu, C.; Hu, X.; Wu, X.; Yang, Y.; Tian, H., Halogen chemistry of solid electrolytes in all-solid-state batteries. *Nat. Rev. Chem.* **2023**, 1-17.

9. Vu, T. T.; Cheon, H. J.; Shin, S. Y.; Jeong, G.; Wi, E.; Chang, M., Hybrid electrolytes for solid-state lithium batteries: Challenges, progress, and prospects. *Energy Storage Mater.* **2023,** *61*, 102876.

10. Manthiram, A.; Yu, X.; Wang, S., Lithium battery chemistries enabled by solid-state electrolytes. *Nat. Rev. Mater.* **2017,** *2* (4), 1-16.

11. Tang, H.; Deng, Z.; Lin, Z.; Wang, Z.; Chu, I.-H.; Chen, C.; Zhu, Z.; Zheng, C.; Ong, S. P., Probing solid–solid interfacial reactions in all-solid-state sodium-ion batteries with first-principles calculations. *Chem. Mater.* **2018,** *30* (1), 163-173.

12. Yao, Y.; Kummer, J., Ion exchange properties of and rates of ionic diffusion in beta-alumina. *J. Inorg. Nucl. Chem.* **1967,** *29* (9), 2453-2475.

13. Tel'Nova, G.; Solntsev, K., Structure and ionic conductivity of a beta-alumina-based solid electrolyte prepared from sodium polyaluminate nanopowders. *Inorg. Mater.* **2015,** *51*, 257-266.

14. Hong, H.; Kafalas, J.; Goodenough, J., Fast Na^+-ion transport in skeleton structures. *Mater.*

Res. Bull. **1976,** *11* (2), 203-220.

15. Auborn, J.; Johnson Jr, D., Conductivity of Nasicon ceramic membranes in aqueous solutions. *Solid State Ionics* **1981,** *5*, 315.

16. Zhang, Z.; Wenzel, S.; Zhu, Y.; Sann, J.; Shen, L.; Yang, J.; Yao, X.; Hu, Y.-S.; Wolverton, C.; Li, H., $Na_3Zr_2Si_2PO_{12}$: a stable Na^+-ion solid electrolyte for solid-state batteries. *ACS Appl. Energy Mater.* **2020,** *3* (8), 7427-7437.

17. Nonemacher, J. F.; Naqash, S.; Tietz, F.; Malzbender, J., Micromechanical assessment of Al/Y-substituted NASICON solid electrolytes. *Ceram. Int.* **2019,** *45* (17), 21308-21314.

18. Luo, J.; Zhao, G.; Qiang, W.; Huang, B., Synthesis of Na ion‐electron mixed conductor $Na_3Zr_2Si_2PO_{12}$ by doping with transition metal elements (Co, Fe, Ni). *J. Am. Ceram. Soc* **2022,** *105* (5), 3428-3437.

19. Ran, L.; Baktash, A.; Li, M.; Yin, Y.; Demir, B.; Lin, T.; Li, M.; Rana, M.; Gentle, I.; Wang, L.; Searles, D. J.; Knibbe, R., Sc, Ge co-doping NASICON boosts solid-state sodium ion batteries' performance. *Energy Storage Mater.* **2021,** *40*, 282-291.

20. Gao, Z.; Yang, J.; Li, G.; Ferber, T.; Feng, J.; Li, Y.; Fu, H.; Jaegermann, W.; Monroe, C. W.; Huang, Y., TiO_2 as Second Phase in $Na_3Zr_2Si_2PO_{12}$ to Suppress Dendrite Growth in Sodium Metal Solid‐State Batteries. *Adv. Energy Mater.* **2022,** *12* (9), 2103607.

21. Hitesh, B.; Sil, A., Effect of sintering and annealing on electrochemical and mechanical characteristics of $Na_3Zr_2Si_2PO_{12}$ solid electrolyte. *J. Am. Ceram. Soc.* **2023**, 1–12.

22. Zhao, Y.; Goncharova, L. V.; Lushington, A.; Sun, Q.; Yadegari, H.; Wang, B.; Xiao, W.; Li, R.; Sun, X., Superior Stable and Long Life Sodium Metal Anodes Achieved by Atomic Layer Deposition. *Adv. Mater.* **2017,** *29* (18), 1606663.

23. Wan, H.; Mwizerwa, J. P.; Qi, X.; Liu, X.; Xu, X.; Li, H.; Hu, Y. S.; Yao, X., Core-Shell Fe(1-x)S@Na(2.9)PS(3.95)Se(0.05) Nanorods for Room Temperature All-Solid-State Sodium Batteries with High Energy Density. *ACS Nano* **2018,** *12* (3), 2809-2817.

24. Wan, H.; Weng, W.; Han, F.; Cai, L.; Wang, C.; Yao, X., Bio-inspired Nanoscaled Electronic/Ionic Conduction Networks for Room-Temperature All-Solid-State Sodium-Sulfur Battery. *Nano Today* **2020,** *33*, 100860.

25. Liu, G.; Sun, X.; Yu, X.; Weng, W.; Yang, J.; Zhou, D.; Xiao, R.; Chen, L.; Yao, X., $Na_{10}SnSb_2S_{12}$: A nanosized air-stable solid electrolyte for all-solid-state sodium batteries. *Chem. Eng. J.* **2021,** *420*, 127692.

26. Wan, H.; Mwizerwa, J. P.; Han, F.; Weng, W.; Yang, J.; Wang, C.; Yao, X., Grain-boundary-resistance-less Na_3SbS_4-Se solid electrolytes for all-solid-state sodium batteries. *Nano Energy* **2019,** *66*, 104109.

27. Monroe, C.; Newman, J., The impact of elastic deformation on deposition kinetics at lithium/polymer interfaces. *J. Electrochem. Soc* **2005,** *152* (2), A396.

28. Cheng, E. J.; Sharafi, A.; Sakamoto, J., Intergranular Li metal propagation through polycrystalline $Li_{6.25}Al_{0.25}La_3Zr_2O_{12}$ ceramic electrolyte. *Electrochim. Acta* **2017,** *223*, 85-91.

29. Zhao, J.; Tang, Y.; Dai, Q.; Du, C.; Zhang, Y.; Xue, D.; Chen, T.; Chen, J.; Wang, B.; Yao, J., In situ observation of Li deposition‐induced cracking in garnet solid electrolytes. *Energy Environ. Mater.* **2022,** *5* (2), 524-532.

30. Inada, R.; Yasuda, S.; Hosokawa, H.; Saito, M.; Tojo, T.; Sakurai, Y., Formation and stability of interface between garnet-type Ta-doped $Li_7La_3Zr_2O_{12}$ solid electrolyte and lithium metal electrode. *Batteries* **2018,** *4* (2), 26.

31. Liu, X.; Garcia, R.; Lupini, A. R.; Cheng, Y.; Hood, Z. D.; Han, F.; Sharafi, A.; Idrobo, J. C.; Dudney, N. J.; Wang, C., Local electronic structure variation resulting in Li 'filament' formation within solid electrolytes. *Nat. Mater.* **2021,** *20* (11), 1485-1490.

32. Kravchyk, K. V.; Karabay, D. T.; Kovalenko, M. V., On the feasibility of all-solid-state batteries with LLZO as a single electrolyte. *Sci. Rep.* **2022,** *12* (1), 1177.

33. Raj, R.; Wolfenstine, J., Current limit diagrams for dendrite formation in solid-state electrolytes for Li-ion batteries. *J. Power Sources* **2017,** *343*, 119-126.

34. Ke, X.; Wang, Y.; Ren, G.; Yuan, C., Towards rational mechanical design of inorganic solid electrolytes for all-solid-state lithium ion batteries. *Energy Storage Mater.* **2020,** *26*, 313-324.

35. Naranjo, J. M.; Martínez, C. S.; Pandit, B.; Várez, A., High performance NASICON ceramic electrolytes produced by tape-casting and low temperature hot-pressing: Towards sustainable all-solid-state sodium batteries operating at room temperature. *J. Eur. Ceram. Soc.* **2023,** *43* (11), 4826-4836.

36. Min, K., High-Throughput Ab Initio Investigation of the Elastic Properties of Inorganic Electrolytes for All-Solid-State Na-Ion Batteries. *J. Electrochem. Soc.* **2021,** *168* (3), 030541.

37. Wang, T.; Zhang, M.; Zhou, K.; Wang, H.; Shao, A.; Hou, L.; Wang, Z.; Tang, X.; Bai, M.; Li, S.; Ma, Y., A Hetero‐Layered, Mechanically Reinforced, Ultra‐Lightweight Composite Polymer Electrolyte for Wide‐Temperature‐Range, Solid‐State Sodium Batteries. *Adv. Funct. Mater.* **2023,** *33* (22), 2215117.

38. Wolfenstine, J.; Go, W.; Kim, Y.; Sakamoto, J., Mechanical properties of NaSICON: a brief review. *Ionics* **2022,** *29* (1), 1-8.

39. Wang, X.; Liu, Z.; Tang, Y.; Chen, J.; Wang, D.; Mao, Z., Low temperature and rapid microwave sintering of $Na_3Zr_2Si_2PO_{12}$ solid electrolytes for Na-Ion batteries. *J. Power Sources* **2021,** *481*, 228924.

40. Shindrov, A. A., Increasing sinterability and ionic conductivity of $Na_3Zr_2Si_2PO_{12}$ ceramics by high energy ball-milling. *Solid State Ionics* **2023,** *391*, 116139.

41. Niazmand, M.; Khakpour, Z.; Mortazavi, A., Electrochemical properties of nanostructure NASICON synthesized by chemical routes: A comparison between coprecipitation and sol-gel. *J. Alloys Compd.* **2019,** *798*, 311-319.

42. Lee, J. S.; Chang, C. M.; Lee, Y. I.; Lee, J. H.; Hong, S. H., Spark plasma sintering (SPS) of NASICON ceramics. *J. Am. Ceram. Soc.* **2004,** *87* (2), 305-307.

43. Wang, H.; Okubo, K.; Inada, M.; Hasegawa, G.; Enomoto, N.; Hayashi, K., Low temperature-densified NASICON-based ceramics promoted by Na_2O-Nb_2O_5-P_2O_5 glass additive and spark plasma sintering. *Solid State Ionics* **2018,** *322*, 54-60.

44. Lalère, F.; Leriche, J.; Courty, M.; Boulineau, S.; Viallet, V.; Masquelier, C.; Seznec, V., An all-solid state NASICON sodium battery operating at 200 °C. *J. Power Sources* **2014,** *247*, 975-980.

45. Yang, Z.; Tang, B.; Xie, Z.; Zhou, Z., NASICON‐type $Na_3Zr_2Si_2PO_{12}$ solid‐state electrolytes for sodium batteries. *ChemElectroChem* **2021,** *8* (6), 1035-1047.

46. Li, Y.; Sun, Z.; Yuan, X.; Jin, H.; Zhao, Y., NaBr-Assisted Sintering of $Na_3Zr_2Si_2PO_{12}$ Ceramic Electrolyte Stabilizes a Rechargeable Solid-state Sodium Metal Battery. *ACS Appl. Mater. Interfaces* **2023,** *15* (42), 49321-49328.

47. Suzuki, K.; Noi, K.; Hayashi, A.; Tatsumisago, M., Low temperature sintering of $Na_{1+x}Zr_2Si_xP_{3-x}O_{12}$ by the addition of Na_3BO_3. *Scr. Mater.* **2018,** *145*, 67-70.

48. Ji, Y.; Honma, T.; Komatsu, T., Synthesis and Na^+ ion conductivity of stoichiometric $Na_3Zr_2Si_2PO_{12}$ by liquid-phase sintering with $NaPO_3$ glass. *Materials* **2021,** *14* (14), 3790.

49. Oh, J. A. S.; He, L.; Plewa, A.; Morita, M.; Zhao, Y.; Sakamoto, T.; Song, X.; Zhai, W.; Zeng, K.; Lu, L., Composite NASICON ($Na_3Zr_2Si_2PO_{12}$) solid-state electrolyte with enhanced Na^+ ionic conductivity: effect of liquid phase sintering. *ACS Appl. Mater. Interfaces* **2019,** *11* (43), 40125-40133.

50. Li, Y.; Sun, Z.; Jin, H.; Zhao, Y., Engineered Grain Boundary Enables the Room Temperature Solid-State Sodium Metal Batteries. *Batteries* **2023,** *9* (5), 252.

51. Li, W.; Zhao, N.; Bi, Z.; Guo, X., Insight into synergetic effect of bulk doping and boundary engineering on conductivity of NASICON electrolytes for solid-state Na batteries. *Appl. Phys. Lett.* **2022,** *121* (3), 033901.

52. Zhang, Z.; Shi, S.; Hu, Y.; Chen, L., Sol-gel synthesis and conductivity properties of sodium ion solid state electrolytes $Na_3Zr_2Si_2PO_{12}$. *J. Inorg. Mater.* **2013,** *28*, 1255-1260.

53. Zhang, L.; Liu, Y.; Han, J.; Yang, C.; Zhou, X.; Yuan, Y.; You, Y., Al Doped into Si/P Sites of $Na_3Zr_2Si_2PO_{12}$ with Conducted Na_3PO_4 Impurities for Enhanced Ionic Conductivity. *ACS Appl. Mater. Interfaces* **2023,** *15* (38), 44867-44875.

54. Ignaszak, A.; Pasierb, P.; Gajerski, R.; Komornicki, S., Synthesis and properties of Nasicon-type materials. *Thermochim. Acta* **2005,** *426* (1-2), 7-14.

55. Gordon, R.; Miller, G.; McEntire, B.; Beck, E.; Rasmussen, J., Fabrication and characterization of Nasicon electrolytes. *Solid State Ionics* **1981,** *3*, 243-248.

56. Park, H.; Kang, M.; Park, Y.; Jung, K.; Kang, B., Improving ionic conductivity of Nasicon ($Na_3Zr_2Si_2PO_{12}$) at intermediate temperatures by modifying phase transition behavior. *J. Power Sources* **2018,** *399*, 329-336.

57. Jaschin, P. W.; Tang, C. R.; Wachsman, E. D., High-rate cycling in 3D dual-doped NASICON architectures toward room-temperature sodium-metal-anode solid-state batteries. *Energy Environ. Sci.* **2024,** *17* (2), 727-737.

58. Jolley, A. G.; Cohn, G.; Hitz, G. T.; Wachsman, E. D., Improving the ionic conductivity of NASICON through aliovalent cation substitution of $Na_3Zr_2Si_2PO_{12}$. *Ionics* **2015,** *21*, 3031-3038.

59. Lu, Y.; Li, L.; Zhang, Q.; Niu, Z.; Chen, J., Electrolyte and Interface Engineering for Solid-State Sodium Batteries. *Joule* **2018,** *2* (9), 1747-1770.

60. Mohtadi, R.; Orimo, S., The renaissance of hydrides as energy materials. *Nat. Rev. Mater.* **2016,** *2* (3), 1-15.

61. Yoshida, K.; Sato, T.; Unemoto, A.; Matsuo, M.; Ikeshoji, T.; Udovic, T. J.; Orimo, S.-i., Fast sodium ionic conduction in $Na_2B_{10}H_{10}$-$Na_2B_{12}H_{12}$ pseudo-binary complex hydride and application to a bulk-type all-solid-state battery. *Appl. Phys. Lett.* **2017,** *110* (10), 103901.

62. Yan, G.; Yu, S.; Nonemacher, J. F.; Tempel, H.; Kungl, H.; Malzbender, J.; Eichel, R.-A.; Krüger, M., Influence of sintering temperature on conductivity and mechanical behavior of the solid electrolyte LATP. *Ceram. Int.* **2019,** *45* (12), 14697-14703.

63. Kim, Y.; Jo, H.; Allen, J. L.; Choe, H.; Wolfenstine, J.; Sakamoto, J.; Pharr, G., The Effect of Relative Density on the Mechanical Properties of Hot‐Pressed Cubic $Li_7La_3Zr_2O_{12}$. *J. Am. Ceram. Soc.* **2016,** *99* (4), 1367-1374.

64. Zinkevich, T.; Fiedler, A.; Guin, M.; Tietz, F.; Guillon, O.; Ehrenberg, H.; Indris, S., Na^+ ion mobility in $Na_{3+x}Sc_2(SiO_4)x(PO4)_{3-x}(0.1< x< 0.8)$ observed by 23Na NMR spectroscopy. *Solid state ionics* **2020,** *348*, 115277.